Binding of Phenylphosphocholine−Carrier Conjugates to the Combining Site of Antibodies Maintains a Conformation of the Hapten†

Elisar Barbar,‡,§ Tammy M. Martin,|| McKay Brown,|| Marvin B. Rittenberg,*,|| and David H. Peyton*,‡

Department of Chemistry, Portland State University, Portland, Oregon 97207-0751, and Department of Molecular Microbiology and Immunology, Oregon Health Sciences University, Portland, Oregon 97201

Received April 12, 1995; Revised Manuscript Received December 11, 1995⊗

ABSTRACT: The structural basis of the binding of phenylphosphocholine haptens to antibodies was studied. This was done by preparing antibodies and testing binding to conjugates of phenylphosphocholine. The choice of haptens was made in order to evaluate the contribution of the carrier to binding, and its effect on hapten conformation in the active site. Thus, phosphocholine (PC) was diazophenyl-linked to tyrosine or histidine as single amino acid carriers and to tripeptides or octapeptides containing tyrosine or histidine as central amino acids to which PC was attached. Relative affinity was assessed by inhibition enzyme-linked immunosorbent assay (ELISA) and binding constants were determined by fluorescence quenching. Fluorinated haptens were used to determine the kinetics of binding using ^{19}F nuclear magnetic resonance. The transferred nuclear Overhauser effect was used to characterize conformation of the bound hapten. We had previously shown that nitrophenylphosphocholine unlinked to carrier is bound in the active site as a bent structure [Bruderer, U., Peyton, D. H., Barbar, E., Fellman, J. H., & Rittenberg, M. B. (1992) *Biochemistry 31*, 584−589]. We show here that this same bent conformation is retained in the active site regardless of the neighboring carrier or the conformation of the hapten in the unbound conjugate. The presence of the carrier residues in the bound state does, however, influence affinity.

In order to elicit a humoral immune response, most small-molecule haptens must be coupled to protein carriers. It has been documented that protein carriers are internalized, processed to peptides, and presented on the surface of the B cell, where they induce T lymphocyte help to drive further the B cell response (Lanzavecchia, 1990). Internalization requires an initial interaction between the hapten−carrier conjugate and the membrane-bound antibody on the B cell surface. The contribution of the carrier to the initial interaction between ligand and B cell receptor remains unknown. Furthermore, procedures used to produce hapten−carrier protein conjugates usually yield heterogeneous products, with multiple hapten units bound per carrier molecule. While this approach is advantageous for effective induction of antibody, it disallows determination of specific structural details of antigen−antibody interactions.

Many structural studies of antigen−antibody interactions have focused on changes in the conformation of the hapten upon binding (Glaudemans et al., 1990; Anglister & Naider, 1991; Cheetham et al., 1991). Additional studies have emphasized structural dynamics of the antibody itself (Theriault et al., 1991; Constantine et al., 1993a,b). For example, the result of heavy (H-) chain CDR3−hapten interactions in an anti-dansyl antibody was found to include a decrease in H-chain CDR3 internal motion, and the formation of a hydrophobic core comprising two H-chain CDR3 tyrosines and the dansyl ring (Odaka et al., 1992; Takahashi et al., 1992). Another significant finding is that the antibody may, in some cases, exist as an equilibrium of at least two conformations; ligands may bind preferentially to only one of these forms (Foote & Milstein, 1994). It has also been shown that antibody binding can induce changes in a protein antigen that are distant from the structural epitope (Benjamin et al., 1992). While these studies have provided useful information about antigen−antibody interactions at the molecular level, the carrier contribution remains to be tested. Therefore, we have sought to analyze the carrier contribution to hapten binding by utilizing small, homogeneous amino acid−hapten conjugates.

The hapten phosphocholine (PC)[1] is immunogenic when coupled to protein carriers such as keyhole limpet hemocyanin (Claflin et al., 1974; Gearhart et al., 1975; Chang & Rittenberg, 1981). In the BALB/c mouse, virtually all of the antibody in the primary response has high specificity for the PC hapten. However, in the memory response a second anti-PC population emerges which recognizes PC including its phenyl linkage to the protein carrier (Chang et al., 1982). We previously showed that the phenyl-PC hapten NPPC has a bent conformation, both free in solution and when bound to antibody (Bruderer et al., 1992). Furthermore, the phenyl-

† This work was supported in part by a grant from the Oregon Affiliate of the American Heart Association to D.H.P., NIH Grants AI14985 and AI26827 to M.B.R., and Training Grant EY07123 to T.M.M.

* To whom correspondence should be addressed.

‡ Portland State University.

§ Present address: Department of Biochemistry, University of Minnesota, St. Paul, MN 55108.

|| Oregon Health Sciences University.

⊗ Abstract published in *Advance ACS Abstracts,* February 15, 1996.

[1] Abbreviations: Ac, acetyl; TFA, trifluoromethyl; PC, phosphocholine; NPPC, *p*-nitrophenylphosphocholine; NPDBP, *p*-nitrophenyl 3,3-dimethylbutyl phosphate; FPPC, *p*-fluorophenylphosphocholine; TFPPC, *p*-trifluoromethylphenylphosphocholine; CDR, complementarity-determining region; VH, variable region gene−heavy chain; VL, variable region gene−light chain; PC-KLH, phosphocholine−keyhole limpet hemocyanin; DQF-COSY, double-quantum filtered two-dimensional *J*-correlated spectroscopy; NMR, nuclear magnetic resonance; NOE, nuclear Overhauser effect; ROESY, rotating-frame Overhauser effect spectroscopy; sFv, the recombinant single-chain variable fragment of antibody which binds antigen; TOCSY, two-dimensional total correlation spectroscopy; TRNOE, transferred nuclear Overhauser effect; 1D, one-dimensional; 2D, two-dimensional; ELISA, enzyme-linked immunosorbent assay; I_{50}, concentration of hapten (micromolar) required to inhibit antibody binding to phosphocholine−histone by 50% in an enzyme-linked immunosorbent assay.

0006-2960/96/0435-2958$12.00/0

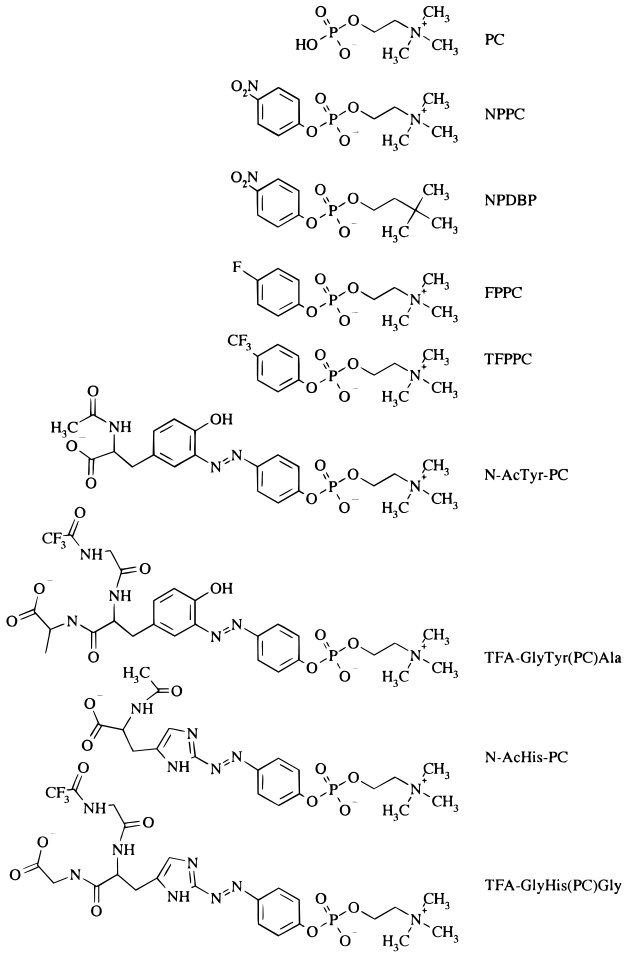

FIGURE 1: Structures of the small molecule hapten-carrier molecules used in this study.

PC hapten analog *p*-nitrophenyl 3,3-dimethylbutyl phosphate (NPDBP), which lacks the positively charged nitrogen, was shown to be in the same bent conformation when bound in the active site but not when it was free in solution, where its structure was not ordered. Thus the antibody could be viewed as selecting and stabilizing a particular (probably minor) conformation from a population of solution structures.

In the present study we extended the structural analysis of phenyl-PC haptens to assess the contribution of the carrier protein to antibody binding. We synthesized a series of haptenated carriers made from amino acids and peptides; the structures of these are shown in Figure 1. The antibody affinity for hapten was shown to be modulated by the identity of the carrier molecule. The bound conformations of at least some of the carriers [N-AcTyr-PC and TFA-GlyTyr(PC)-Ala] were found to be influenced by antibody. ^{19}F NMR of fluorinated haptens resembling NPPC allowed determination of binding kinetics between hapten and the antibodies. From these data, the interconversion between the free and bound ligand was found to be rapid enough to render TRNOE analysis possible. The TRNOE analyses were then performed to find bound-state structures for several of the hapten−carrier conjugates. These results demonstrate that the conformation of the bound hapten is unaffected by the associated carrier residues, although the latter may affect the affinity.

MATERIALS AND METHODS

Syntheses of Haptens. The ligand NPPC was obtained from Sigma. NPDBP was synthesized as described (Brudererer et al., 1989). FPPC and TFPPC were prepared as described below, using modifications of procedures for producing the phosphate esters (Turner & Khorana, 1959) and choline substitution (Chesebro & Metzger, 1972).

(A) p-Fluorophenylphosphocholine (FPPC). *p*-Fluorophenol (10 g, Aldrich) was treated with excess aqueous NaOH to form sodium *p*-fluorophenoxide, which was filtered and dried over phosphorus pentoxide at reduced pressure. The resulting 5 g of solid was slowly added to phosphorus oxychloride (Aldrich) under dry N_2 at 0 °C. The vigorous reaction was moderated by cooling in an ice bath. When addition was complete, solid NaCl was removed by vacuum filtration, and unreacted phosphorus oxychloride was removed by rotary evaporation. The resulting oil was distilled in a short-path apparatus at 30 μm with a boiling point range of 91−105 °C; yield (*p*-fluorophenyl phosphodichloridate) 0.85 g.

Choline iodide (1 g) and 516 μL dry quinoline were added to the *p*-fluorophenyl phosphodichloridate (0.85 g) in 3 mL of dry acetonitrile and stirred at 0 °C in the dark for 8 h. Pyridine (2.0 mL) and 400 μL of water were then added, and the solution was incubated at room temperature for 2 h. The solvents were removed by rotary evaporation. The viscous residue was then dissolved in 10 mL of water, and the pH was adjusted to 7. The solution was passed through a 70-mL TMD-8 mixed-bed resin (Sigma) column preequilibrated with water. The pooled eluate was lyophilized to give 110 mg of white crystals. The product was analyzed on Analtech thin-layer cellulose plates using the mobile phase isopropyl alcohol/ammonia/water (7:2:1 by volume), which gave a single component as detected by fluorescence quenching. The product was also checked for purity by ^{1}H, ^{19}F, and ^{31}P NMR. The ^{19}F spectrum showed the expected multiplet (triplet of a triplet of a doublet, with coupling constants 7, 4, and 1.8 Hz) due to coupling from the ^{31}P, in addition to the 2,6- and 3,5-ring protons. Both proton-coupled and proton-decoupled ^{31}P spectra were obtained. The ^{1}H-decoupled spectrum showed a doublet of 1.8 Hz, arising from long-range coupling from the ^{19}F nucleus. The ^{1}H-decoupled ^{19}F spectrum showed only the doublet from coupling to the ^{31}P nucleus. Taken together, these results confirmed that the authentic FPPC had been synthesized and was free of unwanted proton-containing impurities to at least 95%.

(B) Trifluorophenylphosphocholine (TFPPC). TFPPC was prepared the same way as FPPC, with trifluoromethylphenol (Aldrich) as the starting material. The product obtained after mixed-bed chromatography was further purified from free choline by thin-layer chromatography on cellulose plates as above. The final product was analyzed for purity by ^{1}H, ^{19}F, and ^{31}P NMR as outlined above for FPPC, with comparable results.

Synthesis of PC−Amino Acid and PC−Peptide Components. *(A) N-Acetyltyrosinediazophenylphosphocholine (N-AcTyr−PC)*. The amino acids were first N-acetylated because diazonium salts can react with free amino groups (Ahern & Vaughan, 1973). The coupling reaction between N-AcTyr and *p*-diazophenylphosphocholine (DPPC; formed from *p*-aminophenylphosphocholine) was done at alkaline pH with the amino acid in large molar excess (Chesebro & Metzger, 1972). Thus, 0.1 mmol of N-AcTyr (23 mg) was treated with 0.01 mmol (2.82 mg) of *p*-diazophenylphosphocholine (DPPC) in 3 mL of 24 mM borate buffer at pH 9 with stirring at room temperature for 12 h. The pH was then adjusted to 7.0 and the reaction mixture was lyophilized.

The resulting solid was dispersed in methanol and then developed on fluorescent thin-layer cellulose as above, to remove it from unreacted starting material and other impurities. The ^{1}H NMR spectrum of the purified product showed the choline moiety and the characteristic aromatic portion [spin systems AA′BB′ (*phenyl*-PC) and AMN (Tyr)]. The 2D nuclear Overhauser effect spectrum (NOESY) and *J*-correlated spectrum (COSY) led to the assignments of all peaks. The ^{1}H-decoupled ^{31}P NMR spectrum showed the anticipated singlet. Together the NMR results indicated a single molecular species.

(B) TFA-GlyTyr(PC)Ala. Amino-terminal protection was done by treating 50 mg of the tripeptide GlyTyrAla (Sigma) with a 50-fold excess of ethyl trifluorothioacetate (ETFA, Sigma) in 7 mL of borate buffer at pH 9.5 for 10 h with stirring. Excess reagent was removed by rotoevaporation, and then the residue was dissolved and eluted over Sephadex G-10 with water. The protected tripeptide was separated from the unreacted tripeptide by chromatography on Analtech 1000 cellulose TLC plates, developed with an isopropyl alcohol/ammonia/water (7:2:1) mobile phase.

The reaction of N-TFA-GlyTyrAla with DPPC was allowed to proceed as above (with N-AcTyr) with stirring for 8 h at room temperature. The desired PC-monolabeled peptide was purified by thin layer chromatography and analyzed for purity by ^{1}H and ^{31}P NMR. From a COSY spectrum, the Ala and Tyr spin systems were assigned.

(C) N-Acetylhistidinediazophenylphosphocholine (N-AcHis−PC). This molecule was synthesized in the same way as N-AcTyr−PC (above). ^{1}H-decoupled ^{31}P, as well as ^{1}H NMR spectra, showed that the fastest-moving band on the TLC plates was the desired product, which is monolabeled on the ring C_2 position; other bands gave spectra of a hydrolyzed product (phosphate ester cleaved) and a product labeled at both C_2 and C_4 ring positions.

Broadening of peaks in the aromatic region of the ^{1}H NMR spectrum of N-AcHis−PC was noted as evidence of self-association, but only when the N-Ac-His−PC was at high concentration. At the lower concentrations used in the study the spectrum was likely that of a monomer (loss of concentration dependence). The monomer structure was verified by recording the spectrum in 40% acetonitrile-d_3, where the sharper peaks were observed at nearly the same chemical shift as for the low concentration samples.

(D) TFA-GlyHis(PC)Gly. The same procedure as above for TFA-GlyTyr(PC)Ala was followed. Purification was also done as described above for GlyTyr(PC)Ala. Coupling of the His with DPPC introduced a complication (as above for N-acetyl-His−PC) because of the presence of two sites for labeling. This caused lower yield for the monolabeled product, although the spectra confirmed that pure, monolabeled product was obtained.

(E) PC−Octapeptide. The octapeptide Gly-Ala-Gly-Ala-Tyr-Gly-Ala-Gly (Vollum Institute Peptide Synthesis Facility, Oregon Health Sciences University, Portland) was haptenated by essentially the same procedure as above for PC−Tyr. Purification was by reverse-phase HPLC, and characterization of the monohaptenated, N-acetylated product was verified by the expected aromatic-region ^{1}H NMR spectrum.

Synthesis and Expression of Single-Chain Antibody Fragment of M3C65 (sFv). cDNA copies of the VH and VL genes of the phenyl-PC-specific hybridoma M3C65 (Stenzel-Poore & Rittenberg, 1991) were synthesized from mRNA (Fast Track, InVitrogen, San Diego, CA) using random hexamer primers (Pharmacia). PCR amplification (Innis & Gelfand, 1990) was carried out using a primer for the 5′ portion of Vλ1 (5′agatcgcatgccatggGACAGGCTGTTGTGACTCATGGAA-3′) and a primer for the 3′ portion of Jλ1 plus the 5′ part of the $(Gly_4Ser)_3$ linker (5′-cggacccaccaccgcccgagccaccgccaccACCTAGGACAGTCAGTTTGGT-3′). Amplification of the VH M141/D/JH3 gene was carried out using a primer for the 3′ part of the linker plus the 5′VH (5′-tcgggcggtggtgggtccggaggcggatctCAGGTGCAGCTGAAGGAGTCAG-3′) and a primer for the 3′ end of JH3 plus two stop codons and an *Nco*I site (5′-agatcgcatgccatggttatcaTGCAGAGACAGTGACCAGAGTCCC-3′). *Nco*I sites are underlined and V region coding sequences are capitalized. The VH and VL genes were joined by PCR with the linker, $(Gly_4Ser)_3$ (Johnson & Bird, 1991). The amplified sFv DNA was ligated into the *Nco*I site of the pET3d vector (Novagen), sequenced, and transformed into *Escherichia coli* B121-(DE3). Sequencing of the DNA showed that the deduced protein sequence of the sFv region differed from the M3C65 hybridoma at VH amino acid 4, producing an Arg in place of the wild-type Lys. This conservative change had no effect on affinity (Table 2). The induced protein sFv inclusions (24.9 kDa) were denatured and refolded as described (Boss et al., 1984). Renatured sFv fragments were purified by affinity chromatography as described for intact antibody (Chang et al., 1982).

Binding Studies. Hapten inhibition ELISA was performed as described previously (Chang et al., 1982). Briefly, plates were coated with PC−histone and blocked with 1% bovine serum albumin. Purified antibody was preincubated with various concentrations of hapten and then added to the PC−histone-coated plate. Bound antibody was detected with isotype-specific, alkaline phosphatase-conjugated anti-mouse immunoglobulin. Binding percentages were calculated by comparing the sample optical density values (at 410 nm) to antibody standards (without hapten) on the same plate. I_{50} values correspond to the hapten concentration needed to inhibit 50% of the antibody binding to PC−histone.

Determination of binding constants by fluorescence quenching was done on a Perkin-Elmer LS50B luminescence spectrometer at 25 °C. The excitation and emission wavelengths were 295 and 345 nm, respectively. Stock ligand solutions (0.1 mM) were diluted in phosphate-buffered saline (PBS; 137 mM NaCl, 1.6 mM sodium phosphate, 3 mM KCl, and 3 mM NaN_3, pH 7.4) to an appropriate concentration and 25-μL aliquots were added, with stirring, in 10 steps to an initial volume of 2.9 mL of antibody sample at 10^{-8} M. Results were obtained by linear regression analysis of the reciprocal of quenching vs the reciprocal of ligand concentration ($1/Q$ vs $1/[L]$). The binding constant K_a is then equal to the negative of the slope of a Scatchard plot (r/L vs r).

NMR Spectroscopy. The antibodies for NMR analysis were in 400 μL of deuterated PBS buffer. A typical NMR sample contained 450 μL of 40 μM intact antibody. The molar ratios of ligand to antibody were 50:1 unless otherwise stated. The protein solution was concentrated by ultrafiltration and then exchanged into D_2O-based PBS buffer to reduce the water signal. After each hapten was studied, the sFv or intact antibody was purified by gel filtration. Typical protein concentrations were 0.1−0.7 mM for the sFv and 40 μM for the antibody.

Table 1: Fine Specificity of Anti-phenyl-PC Antibodies for PC-Based Ligands, Determined by ELISA[a]

	ligand						
antibody	NPPC	FPPC	TFPPC	N-AcTyr-PC	N-AcHis-PC	TFA-GlyTyr(PC)Ala	TFA-GlyHis(PC)Gly
PCG1-1	35 ± 20[b]	80 ± 10	43 ± 15	3 ± <1	9 ± <1	13 ± 3	60 ± 1
M3C65	170 ± 90	640 ± 20	>500	5 ± <1	20 ± 10	11 ± 7	150 ± 50
PCG1-2	3100 ± 600	>1000	>500	140 ± 60	350 ± 120	14 ± 4	170 ± 30

[a] I_{50} values: concentrations of hapten (micromolar) required to inhibit antibody binding to PC−histone by 50% in an ELISA. [b] Deviations are the ranges of two or more determinations, each performed in triplicate.

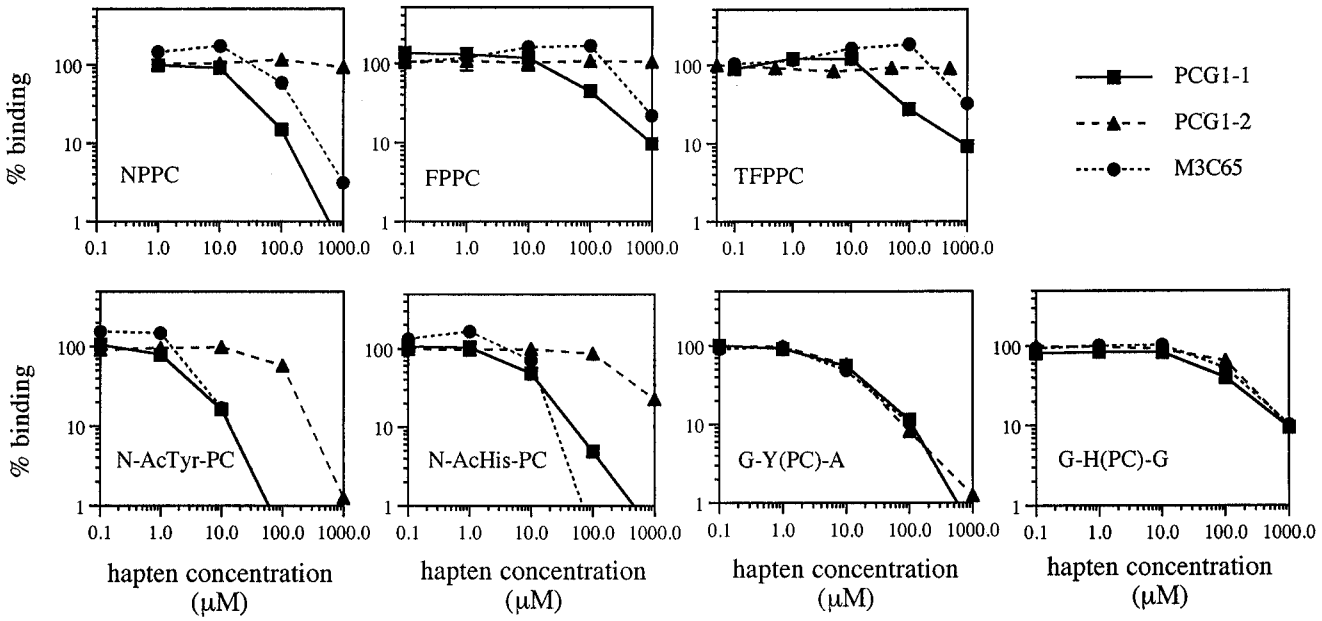

FIGURE 2: Binding inhibition curves from which the I_{50} values were determined. Optical density values for each antibody in the absence of competing hapten were set at 100% binding. All experiments were performed two or more times (each in triplicate). Data points represent averages except for TFPPC and TFA-GlyHis(PC)Gly because they were repeated using slightly different hapten concentrations. The plots for these cases are representative single determinations.

All NMR spectra were performed on a Bruker AMX-400 spectrometer in the phase-sensitive mode. Chemical shifts were referenced to 2,2-dimethyl-2-silapentane-5-sulfonate through the residual water signal. Transferred NOESY spectra were acquired at 80-, 100-, and 300-ms mixing times. Some of the NOESY spectra of the sFv/haptens at near 1:4 molar ratios were recorded at 70-ms mixing time. The residual solvent line was presaturated using low power during the 2-s relaxation delay. The carrier frequency was placed at the HDO resonance in all the experiments. The data were acquired with a spectral window of 4808 Hz. At least 242 t_1 values were obtained, and free induction decays for t_2 were recorded in 1024-point blocks, summing at least 84 acquisitions each. The data sets were zero-filled to give either a 512 × 1024 or a 1024 × 1024 data matrix after Fourier transformation. The NOESY (Kumar et al., 1980), ROESY (Bothner-By et al., 1984; Bax & Davis, 1985), DQF-COSY (Rance et al., 1983), and TOCSY (Braunchweiler & Ernst, 1983) spectra were recorded in the phase-sensitive mode using the time-proportional phase incrementation (TPPI) method (Marion & Wüthrich, 1983). Routine ^{19}F and ^{31}P spectra were recorded without ^{1}H-decoupling unless otherwise noted. For kinetics studies, 0.08 mM TFPPC hapten was titrated with the sFv to achieve a final 20-fold excess of hapten. A NOESY spectrum for 0.6 mM of the free sFv was obtained with a 70-ms mixing time.

Molecular Modeling and Energy Calculations. Molecular modeling and energy calculations for the amino acid− and tripeptide−PC conjugates were carried out using Spartan version 3.1, running on a Silicon Graphics workstation. The molecular mechanics minimization was performed using the SYBYL force field (Clark et al., 1989) for the conformational search. No correction for solvent effects was applied.

RESULTS

Binding of Anti-phenyl-PC Antibodies by Fluorinated Haptens and Small Amino Acid−PC Conjugates. PC-coupled ligands serving as models for PC-coupled proteins were tested for binding to representative anti-phenyl-PC antibodies by inhibition ELISA (Table 1). For PCG1-1 and PCG1-2, similar I_{50} values were obtained for the fluorinated haptens (FPPC and TFPPC) as for NPPC, indicating that substitution of the nitro group by a fluoro or trifluoromethyl group did not strongly perturb either the ligand or the binding pocket of the antibody. For M3C65, the reduction in TFPPC inhibition compared to NPPC (Table 1) is probably due to weaker hydrogen-bonding interactions of the trifluoromethyl groups (Kooistra & Richards, 1978). Another reason for this decrease might be the difference in geometry between the two groups, spherical for the trifluoromethyl and planar for the nitro group. Similarly, there was only a 2- and 4-fold reduction in FPPC inhibition compared to NPPC for M3C65 and PCG1-1, respectively. The binding curves from these inhibition ELISAs (Figure 2) show that although FPPC and TFPPC inhibit less well than NPPC, the relative order of inhibition (PCG1-1 > M3C65 ≫ PCG1-2) remained consistent. Therefore, replacement of the NO_2 group with either F or CF_3 does not appreciably alter the character of the NPPC hapten, allowing their use in these studies.

Table 2: Binding Constants Determined by Fluorescence Quenching[a]

	ligand				
antibody	NPPC	N-AcTyr-PC	N-AcHis-PC	TFA-GlyTyr(PC)Ala	NPDBP
PCG1-2	(2.5 ± 0.4)[b] $\times 10^4$	$(1.7 \pm 0.1) \times 10^5$	$<2.0 \times 10^4$	*c*	*d*
M3C65	$(3.1 \pm 0.2) \times 10^6$	$(5.1 \pm 0.5) \times 10^7$	$(1.1 \pm 0.3) \times 10^7$	$(6.1 \pm 2.0) \times 10^6$	$(4.4 \pm 0.1) \times 10^4$
M3C65 sFv	$(3.2 \pm 0.2) \times 10^6$	$(5.6 \pm 0.2) \times 10^7$	$(1.3 \pm 0.3) \times 10^7$	$(7.6 \pm 1.7) \times 10^6$	$(4.6 \pm 0.1) \times 10^4$

[a] K_{assoc} (M^{-1}). [b] Averages of two or more determinations ± range. [c] Affinity below level of detection. [d] Not determined: PCG1-2 belongs to a subset of antibodies that bind NPDBP poorly (Bruderer et al., 1989).

For all three antibodies, N-AcTyr−PC inhibited binding 2−4-fold better than N-AcHis−PC. Interestingly, both of the amino acid-containing haptens were better at inhibiting binding than NPPC. Even though NPPC contains the requisite phenyl ring present on the conjugated form of PC, the additional presence of a tyrosine or histidine functional group improves the capability of these haptens to compete for binding of the antibody to the PC−protein on the plates. These ELISA data are consistent with affinity measurements made by fluorescence quenching (Table 2), where the K_a for N-AcTyr−PC was 7−18-fold greater than for NPPC. This is also consistent with a previous report that the addition of a dinitrophenyl group to the aminophenyl residue of NPPC increased the affinity of IgG antibodies from 6- to 80-fold over the affinity for PC alone (Rodwell et al., 1983). N-AcTyr and N-AcHis which were not PC-coupled showed no significant inhibition of binding (data not shown).

As with the unconjugated amino acid haptens, neither the Tyr nor the His tripeptide (without PC attached) inhibited binding, confirming that the phenyl-PC portion was necessary for recognition. The monoclonal M3C65 binds less well to TFA-GlyTyr(PC)Ala than to N-AcTyr−PC, as shown by inhibition binding curves (Figure 2) and affinity measurements (Table 2). This same trend was observed with PCG1-1. The PC−His tripeptide showed some binding by inhibition ELISA, but the I_{50} was reduced by ~7-fold relative to N-AcHis−PC (Table 1). Thus for PCG1-1 and M3C65, the neighboring amino acids reduced binding to the haptenated residue. PCG1-2 (whose K_a for NPPC is approximately 100-fold less than that of M3C65) was inhibited better by both PC−tripeptides than by N-AcTYr−PC or N-AcHis−PC (Table 1), but its affinity for haptenated tripeptide was too low to detect by fluorescence quenching (Table 2). Differences between these two types of determinations have been previously obtained (Brown et al., 1992). Hapten inhibition (I_{50}) is a measure of antibody binding to solid-phase antigen, while fluorescence quenching is a measure of the intrinsic affinity of antibody for free hapten in solution. Finally, we note that NPDBP, lacking the positively charged nitrogen, has a lower binding constant than NPPC for the antibody M3C65 as well as to its sFv (Table 2).

M3C65 sFv Interactions with Models for PC−Protein Conjugates (NMR Analysis). M3C65 is an antibody with a very high affinity for the phenyl-PC haptens (Tables 1 and 2) and so is a logical target for structural study. The high affinity of M3C65 for the phenyl-PC haptens also makes this a particularly suitable case for studying interactions specifically involving the antibody, because one can work at hapten:antibody ratios of near 1:1. This section begins with an evaluation of hapten off rate for the antibody M3C65, and then data are presented that are related to binding interactions between hapten and the antibody.

The approximate rate k_{off} is important, especially when evaluating the effects on NMR spectra (Anglister & Zilber, 1990). The presence of the fluorine nuclei in the TFPPC hapten provided a convenient way for measuring the dissociation rate, k_{off}, ^{19}F NMR is particularly useful for studying ligand−macromolecule interactions because the ^{19}F nucleus is very sensitive to environmental changes (Gerig, 1989). Signals from bound ligands are often detected in ^{19}F spectra because there is less interference from other resonances (Craik & Higgins, 1989; Glaudemans et al., 1990) and because of typically large chemical shift dispersion. The ^{19}F signal was broadened and shifted upfield by 0.1 ppm when bound to the M3C65 sFv (data not shown). Hydrogen bonding and local electronic effects from close aromatic side chains probably gave rise to the chemical shift difference. Using the complete band-shape method (Binsch, 1968; Sandström, 1982), the line broadening of the free resonance induced by chemical exchange yielded a calculation of k_{off} at 140 ± 10 s^{-1} at 25 °C. This titration of the antibody with the ligand was also done with FPPC but no k_{off} rate was determined because of long-range ^{31}P coupling of the ^1H-decoupled ^{19}F signal. However, the general features of line broadening and chemical shift were similar.

The interaction of TFPPC with the M3C65 sFv is further revealed by 1D ^1H NMR. Figure 3 shows spectra of 0.15 mM sFv, both free and with increasing concentrations of TFPPC, and of the free hapten in presence of sFv (difference spectrum F, Figure 3). The aromatic *ortho* protons and the 9-proton δ-methyl singlet [$-N^+(CH_3)_3$] are the most broadened of the hapten resonances. A likely explanation for peaks from the same rigid ring system of the TFPPC phenyl experiencing differential broadening is that, for the more broadened resonances, the bound peak position is more shifted from its free position. This broadening is most evident in difference spectrum E, Figure 3. In addition, there are some perturbations to the sFv resonances when it is bound to TFPPC. These perturbations are most obvious in the 0.5−2 ppm and aromatic regions in trace E, Figure 3.

Next, 2D NMR data are reported that relate to specific interactions between M3C65 and the phenyl-PC haptens. We reported previously that NPPC had a bent conformation both when free in solution and when bound in the active site (Bruderer et al., 1992). This is also true for TFPPC; the 2D NOESY of the bound TFPPC/M3C65 sFv complex has TRNOE cross-peaks indicative of the bent conformation (i.e., between the 9-proton δ-methyl singlet and the phenyl protons). The negative NOEs for the intrahapten TFPPC resonances indicate that the excess free ligand is undergoing chemical exchange with the slowly tumbling complex, and hence the intrahapten NOEs give the conformation of the bound ligand. The M3C65 antibody was also titrated with NPDBP, an analog that is bound by M3C65 sFv (Table 2), to study the effect of the antibody on conformation of the ligand which lacks the N^+. A 30:1 molar excess of the antibody over ligand was used to maximize intrahapten TRNOEs. As indicated above, this hapten has an unstruc-

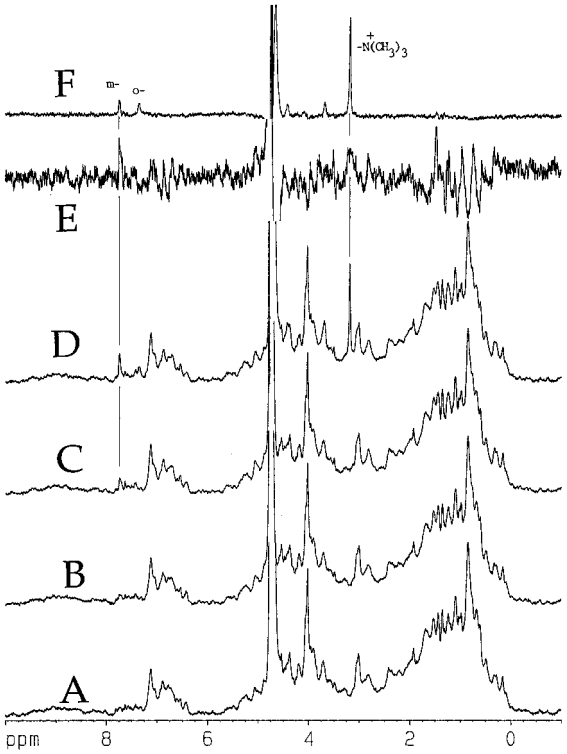

FIGURE 3: ^{1}H NMR spectra showing titration of 0.15 mM sFv of M3C65 with different amounts of TFPPC at pH 7.0 and 25 °C. Molar ratios of TFPPC:sFv are 0:1 (A), 0.5:1 (B), 2:1 (C), and 5:1 (D). (E) is the difference spectrum of (C)−(A); (F) is the difference spectrum of (D)−(C). Therefore, (E) shows changes in the antibody chemical shifts as hapten is added, in addition to some hapten signals. The most broadened hapten resonances are those which have sFv-bound positions most shifted from their free positions. (F) shows the free hapten, with the bound M3C65 sFv removed by subtraction; in this trace the broadening due to exchange is less pronounced than it is in trace (E) because the fraction of free hapten is greater.

tured conformation when free in solution but adopts a bent conformation when bound to PCG1-2 and two other anti-phenyl-PC antibodies (Bruderer et al., 1992). The 1D TRNOE difference spectrum showed negative peaks for hapten aromatic protons upon irradiation of the $C(CH_3)_3$ group (data not shown). This demonstrates proximity in the bound state between the ends of the molecule, indicating that it also is in the bent conformation when bound to M3C65.

There are also NOEs observed between the bound haptens and the sFv (Figure 4A); a few cross-peaks are especially noteworthy. There is a very strong NOESY cross-peak between 3.18 and 1.40 ppm. Figure 4B shows this cross-peak is also present when the ligand is NPDBP; we used this ligand because it lacks the charged nitrogen, and so its 9-proton δ-methyl singlet is at a very different position from that of NPPC and the other PC-based haptens. This resolved a peak-overlap problem; this cross-peak, indicated by an asterisk in Figure 4B, must arise from an intraantibody interaction, at least for the NPDBP case, because unlike NPPC this hapten has no free resonance at 3.18 or 1.40 ppm. A noteworthy and strong cross-peak is present in only the NPDBP/sFv complex spectrum at 0.9 to −0.4 ppm (Figure 4B). This likely represents exchange between free and bound hapten; we are now seeking to establish this conclusion experimentally. The 3.18/1.40 ppm cross-peak in Figure 4A may therefore arise from a combination of NOE and chemical exchange. This nearly 2 ppm upfield shift in the δ-methyl position upon binding to sFv most likely results from ring-current shifts of aromatic rings in the sFv combining site. In the sFv/NPDBP case, the sFv resonance at 1.40 ppm showed an NOE to an aromatic proton at 7.0 ppm which was not observed in the free sFv. The δ and β methylene protons of the choline portion showed NOEs to aromatic protons of the sFv at 6.85 ppm (not shown). These results indicate that the orientation of the choline moiety brings it within 5 Å of an aromatic residue in the combining site.

NMR analyses were performed for other haptens for which binding data were available (Tables 1 and 2) in order to establish whether difference in binding might be due to differences in hapten conformation. NOESY connectivities obtained for the M3C65 sFv/FPPC, sFv/NPPC, sFv/NPDBP, and sFv/N-AcTyr-PC systems were analogous to those described above for the sFv/TFPPC system (data not shown for all of these cases). The bent conformation of the PC end of the bound hapten was also observed for each case. There is also evidence for a conformational change of the sFv upon binding hapten, again analogous to that described above for the sFv/TFPPC system. This is best demonstrated by the strong NOE between two protons of the sFv, at 3.18 and 1.40 ppm (analogous to Figure 4A,B) only when hapten is bound; this NOE does not appear in the free sFv spectrum (Figure 4C).

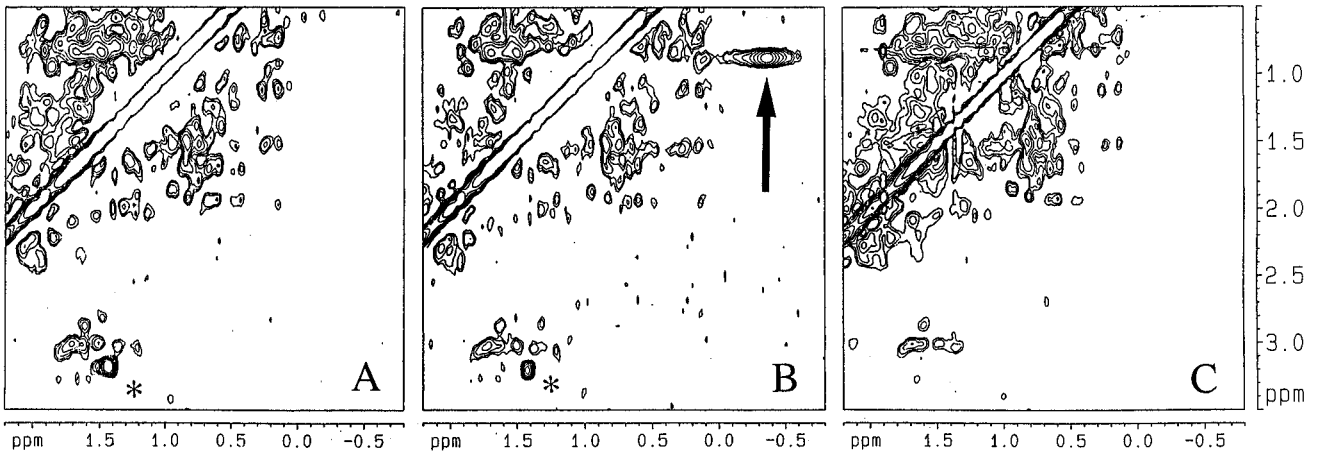

FIGURE 4: Regions from the two-dimensional NOESY spectra of the M3C65 sFv with 5-fold excess of the ligands TFPPC (A) and NPDBP (B). Spectrum (C) is the sFv without added hapten. Spectra were recorded at 25 °C and pH 7.0 with a 70-ms mixing time. In (A) and (B) the strong 3.2/1.4 ppm cross-peaks are indicated with asterisks, and in (B) the strong 0.9/−0.4 ppm cross-peak is indicated with an arrow.

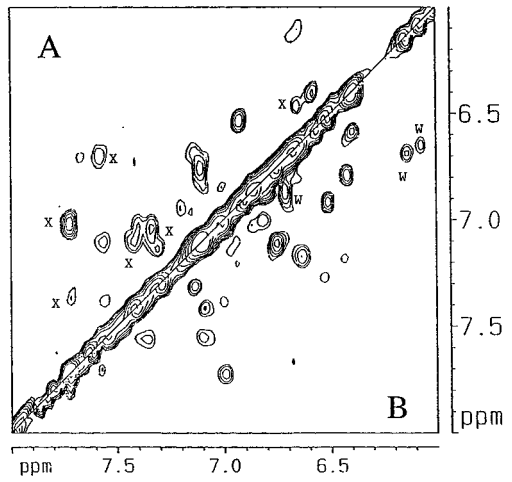

FIGURE 5: NOESY spectra of the aromatic region of FPPC-bound M3C65 sFv (molar ratio 2:1) (A; above the diagonal), and the sFv alone (B; below the diagonal). Spectra were recorded at 25 °C and pH 7.0 with a 70-ms mixing time. Cross-peaks that appear only when FPPC is present, or which have substantially increased intensity, are marked with X; cross-peaks which are more intense or only present in free sFv are marked with W. The aromatic resonances from FPPC are all centered at ≈7.1 ppm and so do not give rise to intrahapten TRNOE cross-peaks.

When a phenyl-PC hapten such as FPPC is added to the M3C65 sFv, the aromatic region NOE pattern changes (Figure 5). FPPC was chosen for this because its aromatic protons were all located at 7.1 ppm, and so the NOE pattern in the aromatic region must arise from sFv protons. Therefore, these changes indicate a change in conformation, and perhaps in flexibility, of the antibody sFv upon binding to hapten. Decreased flexibility of the antibody would lead to an increase in the effective correlation time (which is a summation of all possible motions in the molecule) and would give rise to increased NOEs (Harris, 1986). Some of the cross-peaks are in fact increased, as indicated by Xs in Figure 5. At this point it is difficult, however, to separate effects caused by changes in conformation from effects caused by changes in rigidity. In fact, the analysis is further complicated by a few cross-peaks which either change position substantially or are present only in unbound sFv (indicated by Ws in Figure 5). The dispersive character of the upfield region in Figure 3E demonstrates that changes in peak positions of the sFv also occur in the 0−2 ppm aliphatic region. Figure 3E also shows the dispersive character that results from changes in the aromatic proton chemical shifts that results from hapten binding.

PCG1-2 Antibody Interactions with Models of PC−Protein Conjugates (NMR Analysis). We also studied the interaction of PCG1-2 with the phenyl-PC haptens. PCG1-2 has a lower affinity for the these haptens than does M3C65, and PCG1-2 requires the positive end of the choline for strong binding. The lowered binding affinity generally reflects increased off rates of the haptens and so gives enhanced transferred NOESY cross-peaks relative to M3C65. This allows more facile analysis of bound hapten structures. Furthermore, PCG1-2 is an antibody for which we already have published TRNOEs when bound to the simplest PC−protein model, NPPC (Bruderer et al., 1992).

First, we characterized the hapten−carrier complexes in solution, with no added antibody. This was necessary for a meaningful comparison to the antibody-bound structures. A NOESY spectrum was obtained to determine the structure of the free N-AcTyr-PC (data not shown). From the NOE patterns (i.e., between the 9-proton choline singlet and the phenyl-PC aromatic protons), it was seen that the bent, restricted conformation discussed previously for NPPC (Bruderer et al., 1992) was also present in N-AcTyr−PC. It was also observed that the *N*-acetylmethyl (a result of blocking the free amino group prior to haptenation) did not have NOE cross-peaks to any other protons in this molecule. This leads to the conclusion that this end of the molecule is flexible, having several conformations rather than being fixed in close proximity to any other proton in this molecule in the free state. The NOESY spectrum of the peptide TFA-GlyTyr(PC)Ala showed the characteristic bent conformation of PC−haptens, demonstrated by the presence of NOE cross-peaks between the protons of the choline portion and the aromatic peaks of the phenyl ring (data not shown). ^{1}H NMR spectra of N-AcHis−PC clearly showed that this ligand self-associates readily at high concentration, so a spectrum was obtained in 40% acetonitrile to verify that the monomer was the predominant species at the concentrations used in the antibody samples. Similar to N-AcTyr−PC, the *N*-acetylmethyl showed no significant NOE to any other resonance. The PC portion of this molecule had the bent, restricted conformation, as evidenced by the NOEs between the δ-singlet and the aromatic protons of the PC moiety and by the fact that the ^{31}P triplet was significantly distorted from what it would have been in a molecule without significant conformational restriction (data not shown).

Next, we analyzed the haptens, with different carriers, interacting with PCG1-2. This was done to test for the role of the carrier. Titration of PCG1-2 with N-AcTyr−PC showed strong broadening of the δ-proton signal. Differential and strong broadening was also observed for the hapten aromatic resonances. An example of this differential broadening is shown in the 1D reference traces in Figure 6. These effects, combined with the absence of individual free and bound ligand peaks, indicated that the exchange between free and bound forms was in the fast exchange regime, making TRNOE analysis possible. The measured k_{off} of 140 s^{-1} for the much more tightly bound TFPPC/M3C65 sFv system (above and Table 1) supports this conclusion. Figure 6 is a 2D NOESY spectrum for the N-AcTyr−PC/PCG1-2 system under conditions that give predominantly TRNOEs. One difference between the bound and free N-AcTyr−PC ligand NOEs is the indication of proximity of the acetyl portion to the rest of the hapten molecule in the bound form. This proximity was absent in the unbound state, in that there was no NOE detected from the *N*-acetyl to any of the aromatic protons in the free molecule (see above). Figure 7 gives examples of bent hapten conformations, calculated using the SYBYL force field. The conformer for N-AcTyr−PC (top) is about 3 kcal/mol lower in energy than a similar conformer which would have the acetyl swung away from the choline methyl group and the Tyr ring protons. NOESY spectra of the bound ligand show NOEs between the methyl of the acetyl group to each of the Tyr protons and to both PC-phenyl resonances. The δ-to-phenyl NOEs show that the PC portion also assumes the familiar bent conformation. The lowest energy conformer calculated is consistent with data from the bound ligand, as inferred from the NMR data. Thus the influence of the antibody can be viewed as selecting one stable conformer from among several conformers that exist in the unbound state.

The interactions of PCG1-2 with larger hapten−carrier conjugates were then studied to find any perturbations

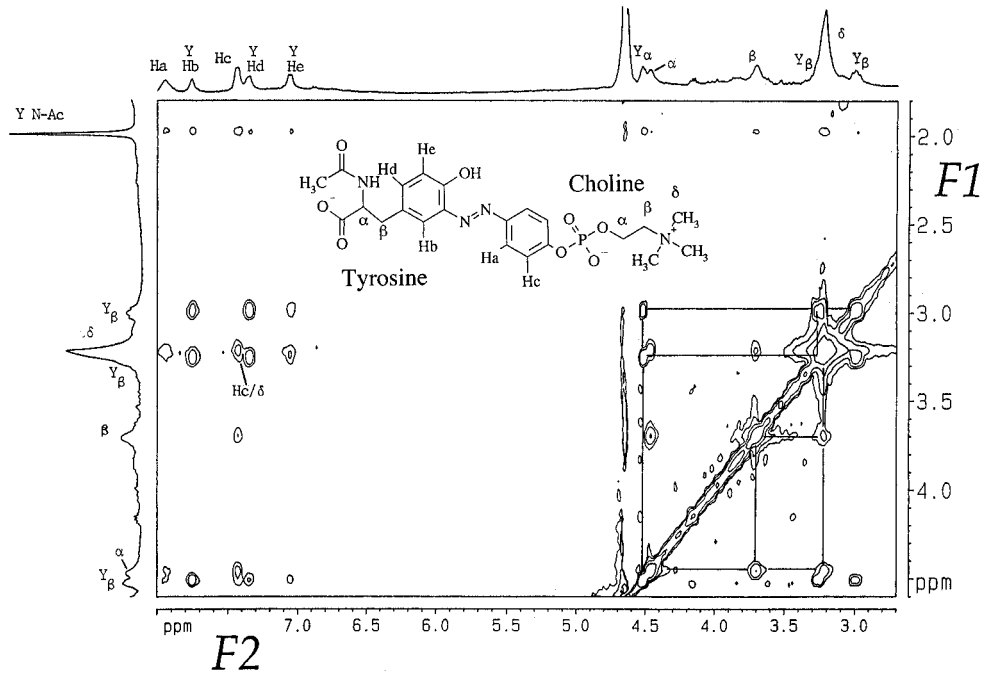

FIGURE 6: TRNOEs shown for 30:1 molar ratio of N-AcTyr-PC with PCG1-2. Correlations in the aliphatic region shown above the diagonal represent cross-peaks between Tyr protons, while correlations in this region below the diagonal show correlations between the PC protons. Tyrosine protons from the hapten are marked Y; choline resonances are as indicated in the structure. This TRNOESY spectrum was recorded at 25 °C and pH 7.0 with a 300-ms mixing time.

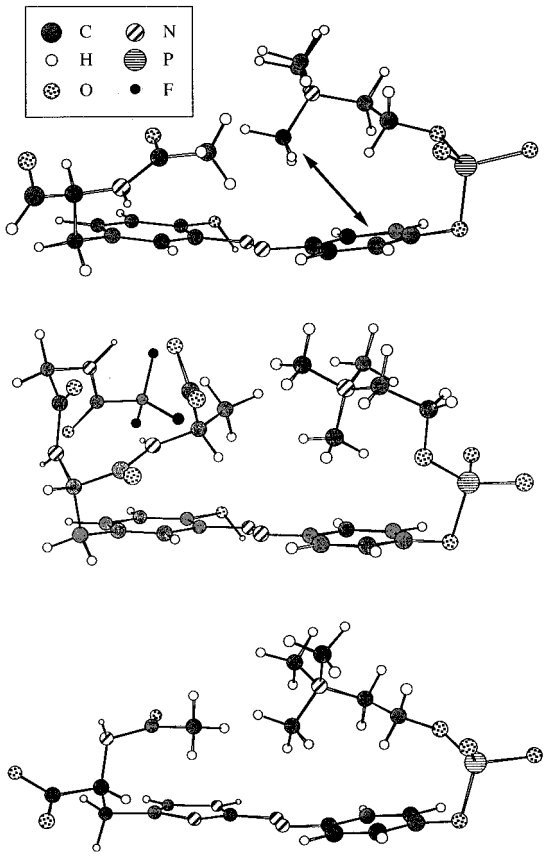

FIGURE 7: Structures of local minimum-energy conformers generated using the SYBYL force field. These structures are consistent (although not necessarily unique) with the bound ligand structural data for N-AcTyr-PC (top), TFA-GlyTyr(PC)Ala (middle), and N-AcHis-PC (bottom). The arrow illustrates the NOEs between the choline 9-proton singlet and phenyl-PC aromatic protons that indicate the bent conformations. The inset gives the symbols for the atoms.

introduced by the increased size and complexity of the carrier. PCG1-2 was titrated with TFA-GlyTyr(PC)Ala (data not shown). At a 12:1 excess of hapten, a sharp methyl doublet started to appear in the 1D spectra, indicating no strong specific interaction with the Ala βCH_3 in the hapten. The bent structure of the phenyl-PC portion was also seen for this case. No NOE cross-peak was observed between the βCH_3 of Ala and the Tyr ring proton; this NOE had been observed in the free peptide, suggesting that a conformational change occurred in the carrier upon binding. Therefore, the Ala βCH_3 distance to the Tyr ring is increased to at least > 5 Å by binding to PCG1-2. Figure 7 (middle) shows the structure of one conformer generated using the SYBYL force field with an energy minimum that is consistent with the bound ligand structure.

The *N*-acetylated, PC-coupled tyrosine octapeptide was examined by DQF-COSY and ROESY in ^1H_2O solvent; resonances were assigned to the four Gly, one Tyr, and three Ala residues (data not shown). The amide and α-protons showed no significant upfield or downfield shifts from their random coil positions, indicating the absence of significant secondary structure. As in the smaller ligands, the hapten moiety in the peptide has the characteristic bent conformation of PC-based haptens, as shown by cross-peaks in the ROESY spectrum between the *ortho* proton of the phenyl ring and the choline protons. The NOESY spectra of the bound complex showed that binding induces a similar conformational change in the antibody as do the other PC-based haptens, shown by the presence of the characteristic strong NOE between two protons of the antibody, at 3.18 and 1.40 ppm, that is observed only in the bound antibody or bound sFv (see Figure 4).

From the DQF-COSY spectrum of the free octapeptide, it was noticed that at least two major different resonance sets exist for the Tyr aliphatic proton spin systems. This implies at least two major conformations for the tyrosine residue. When PCG1-2 was added to the PC−Tyr octapeptide, none of the peaks from the PC−Tyr octapeptide were strongly broadened, indicating that k_{off} must be relatively

slow. This result suggests that the affinity for the octapeptide form of the hapten may be increased over that for N-AcTyr−PC or the PC−Tyr tripeptide. Furthermore and consistent with a slow off rate, TRNOE cross-peaks were not observed and hence could not be used to gain information on the conformation of the bound structure. However, comparison of the COSY spectra of free and bound peptide showed a marked decrease in intensity of the intrahapten cross-peaks due to binding. In the presence of antibody there is only one set of Tyr aliphatic proton cross-peaks, suggesting a single orientation. ROESY data for the free hapten demonstrate a bent conformation for the PC portion.

We now present data on haptens based on coupling phenyl-PC to histidine. This study was done to test the generality of the above effects, but with a different hapten form that could result from the standard protein haptenation procedures (Claflin et al., 1974; Gearhart et al., 1975; Chang & Rittenberg, 1981). PCG1-2 was titrated with N-AcHis−PC (data not shown). At a 5:1 excess of N-AcHis−PC over PCG1-2, a sharp methyl peak at 2 ppm was observed, consistent with little interaction of the antibody with the acetyl end of this molecule, as was also the case for N-AcTyr−PC. The hapten aromatic peaks appeared clearly when the hapten was at 10:1 excess. However, the δ-singlet was broad and did not become readily apparent until the hapten:antibody ratio was 22:1, indicating a large k_{off}. In a NOESY spectrum, the hapten phenyl *meta* protons showed strong NOEs to the *ortho* protons and weaker NOEs to the α, β, and δ protons of the choline, all characteristic of a bent choline conformation. In the free His-PC, the C_4 proton of the imidazole ring showed weak NOEs to the His β-protons. In the bound ligand, this weak NOE disappeared, indicating a possible change in conformation upon binding that increased the distance between the ring C_4 proton and the β-protons to greater than 5 Å, or due to broadening of the C_4 proton peak because of interaction with the antibody, or both. Interaction between hapten and antibody was observed in the form of cross-peaks between the choline β- and δ-protons and an antibody proton at 7 ppm. A strong intraantibody NOE was observed between 3.05 and 1.75 ppm, analogous to that already mentioned for all of the other complexes and consistent with a change in antibody conformation upon hapten binding. Figure 7 (bottom) shows a calculated structure for the N-AcHis−PC conformer with the lowest energy.

DISCUSSION

We undertook these experiments to investigate an elusive aspect of the humoral immune response, namely, the interaction of antibody with the protein portion of the protein−hapten complex necessary to stimulate hapten-specific antibody production. The conditions typically used to make hapten−carrier protein conjugates are often severe and can produce multiply haptenated carriers which are generally heterogeneous and perhaps denatured. We thus decided to produce small hapten−carrier conjugates that are homogeneous and monosubstituted in order to characterize carrier contributions to hapten−antibody interactions.

Our earlier work showed that both the phenylphosphocholine hapten NPPC and its analog NPDBP, which lacks the positively charged nitrogen of choline, have a bent conformation when bound to antibodies, regardless of their free conformation (Bruderer et al., 1992). Each of the PC−carrier molecules reported here retains this characteristic for the hapten when bound. If exchange between bound and free forms of the hapten is fast enough, there can be a strong broadening of specific hapten resonances when in the presence of antibody, especially noticeable in the case of the 9-proton $N(CH_3)_3^+$ resonance from the choline (Figure 6). This broadening is probably due to exchange between the free and bound hapten when there is a large excess of hapten over antibody. That there is a significant chemical shift difference between the free and bound forms for this peak is made likely by the 0.9/−0.4 ppm cross-peak for the M3C65 sFv/NPDBP spectrum in Figure 4B. Furthermore, this broadening is substantially less for more tightly bound cases, such as the TFPPC/M3C65 sFv system in Figure 3F. The differential broadening of the aromatic peaks in bound N-Ac-Tyr−PC is also striking and must result from the specific intermolecular interactions between hapten and antibody. Thus it appears that binding involves specific interactions that change the conformation of both the hapten and antibody. We also note that in the bound complexes, the acetyl CH_3 (from N-terminal blocking) is brought close enough (within 5 Å) to the aromatic portions of the hapten to give NOEs that are not observed in the free molecules. Thus there is a conformational distortion of the carrier as well.

The effect of the carrier on antibody binding is demonstrated by comparison of N-AcTyr−PC and N-AcHis−PC to the larger hapten−carriers. ELISA values (Table 1) demonstrate that N-AcTyr−PC and N-AcHis−PC inhibit binding of representative anti-phenyl-PC antibodies to PC−histone more strongly than NPPC. That is, substitution of the NO_2 moiety by N-AcTyr or N-AcHis makes an energetic contribution to binding. On the other hand, substitution at this position by CF_3 or F diminishes binding considerably. Both of the PC−tripeptides bind more weakly than N-Ac-Tyr−PC and N-AcHis−PC for PCG1-1 or M3C65. It appears that increasing the carrier size diminishes the energetic gain of binding, perhaps because the degrees of freedom of the tripeptides must be reduced to accommodate binding. This loss of entropy of the carrier upon binding diminishes the energetic gain of binding more drastically in flexible small peptides that lack structure than in proteins that are already at low entropy when free. In other words, there is less binding as the size of the carrier peptide is increased until the peptide gains sufficient structure that it does not experience a great loss of entropy upon binding. Results from the octapeptide−PC indicate that the carrier molecule influences conformational averaging and restricts the flexibility of the phenyl-PC hapten. We see two major conformations for the phenyl-PC in the free octapeptide that are interconverting slowly on the NMR time scale, while the smaller carriers showed an average of conformers. We have monolabeled small proteins with PC as models for PC−KLH and we are currently studying the effect of these carriers on both binding and conformations.

Comparing the aromatic region of the bound to the free M3C65 sFv in Figure 5 showed that some cross-peaks gained in intensity. This may be taken as evidence that the residues giving rise to these peaks have diminished flexibility when hapten is bound to the antibody. This loss in flexibility is due to an increased effective correlation time (in this case, probable loss of flexibility of the binding site for hapten), leading to a larger negative NOE (that is, the cross-peaks are in the same phase as the diagonal peaks and have an

increased intensity). Conformational mobility of the antibody combining site has been proposed as a possible mechanism for cross-reactivity and multiphasic binding kinetics (Foote & Milstein, 1994). Such a mechanism may be common. Tyrosine commonly occurs in heavy-chain CDRs, suggesting that this residue is often important to antibody−antigen interaction (Kabat et al., 1987). There are four tyrosine residues in the CDRs of the M3C65 heavy chain. The other aromatic residues in this combinding site are one tryptophan in the heavy chain and two tryptophans, two histidines, and one phenylalanine in the light chain; of these, only the histidine at residue 53 of the light chain has been associated with high-affinity binding (Brown et al., 1992). The likely >1.5 ppm upfield shift of the 9-proton singlet from choline or NPDBP hapten that happens upon binding to sFv certainly implicates interaction with aromatic rings by the ring-current shift mechanism. Work is underway to establish the geometry of the hapten in the antibody combining site.

From the data provided above, it appears that the hapten interacts with the same set of protons of the sFv in all of the ligands studied. These data, coupled with the observation that all of the haptens were in the same bent conformation, suggest that the orientation of the bound PC hapten is similar in all the intact antibodies and antibody fragments studied. The carrier appears to be restricting the mobility in the phenyl-PC region of the PC−carrier peptide complex. Therefore, the differences in I_{50} values and binding affinities of the hapten when coupled to various small carriers are not attributable to changes in the orientation of the hapten in the combining site, but rather to interactions with the carrier.

ACKNOWLEDGMENT

We are indebted to Michael Hare for help in calculating energies for the structures shown in Figure 7.

REFERENCES

Ahern, T. P., & Vaughan, K. (1973) *J. Chem. Soc., Chem. Commun.* 701−702.
Anglister, J., & Zilber, B. (1990) *Biochemistry 29*, 921−928.
Anglister, J., & Naider, F. (1991) *Methods Enzymol. 203*, 228−241.
Bax, A., & Davis, D. G. (1985) *J. Magn. Reson. 65*, 355−360.
Benjamin, D. C., Williams, D. C., Jr., Smith-Gill, S. J., & Rule, G. S. (1992) *Biochemistry 31*, 9539−9545.
Binsch, G. (1968) *Top. Stereochem. 3*, 97−192.
Boss, M. A., Kenten, J. H., Wood, C. R., & Emtage, J. S. (1984) *Nucleic Acids Res. 12*, 3791−3806.
Bothner-By, A. A., Stephens, R. L., Lee, J., Warren, C. D., & Jeanloz, R. W. (1984) *J. Am. Chem. Soc. 106*, 811−813.
Braunchweiler, L., & Ernst, R. R. (1983) *J. Magn. Reson. 53*, 521−528.
Brown, M., Stenzel-Poore, M., Stevens, S., Kondoleon, S. K., Ng, J., Bachinger, H. P., & Rittenberg, M. B. (1992) *J. Immunol. 148*, 339−346.
Bruderer, U., Stenzel Poore, M. P., Bachinger, H. P., Fellman, J. H., & Rittenberg, M. B. (1989) *Mol. Immunol. 26*, 63−71.
Bruderer, U., Peyton, D. H., Barbar, E., Fellman, J. H., & Rittenberg, M. B. (1992) *Biochemistry 31*, 584−589.
Chang, S. P., & Rittenberg, M. B. (1981) *J. Immunol. 126*, 975−980.
Chang, S. P., Brown, M., & Rittenberg, M. B. (1982) *J. Immunol. 129*, 1559−1562.
Cheetham, J. C., Raleigh, D. P., Griest, R. E., Redfield, C., Dobson, C. M., & Rees, A. R. (1991) *Proc. Natl. Acad. Sci. U.S.A. 88*, 7968−7972.
Chesebro, B., & Metzger, H. (1972) *Biochemistry 11*, 766−771.
Claflin, J. L., Lieberman, R., & Davie, J. M. (1974) *J. Immunol., 112*, 1747−1756.
Clark, M., Cramer, R.D., III, & Van Opdensch, N. (1989) *J. Comput. Chem. 10*, 982−1012.
Constantine, K. L., Friedrichs, M. S., Goldfarb, V., Jeffrey, P. D., Sheriff, S., & Mueller, L. (1993a) *Proteins: Struct., Funct., Genet. 15*, 290−311.
Constantine, K. L., Goldfarb, V., Wittekind, M., Friedrichs, M. S., Anthony, J., Ng, S. C., & Mueller, L. (1993b) *J. Biomol. NMR 3*, 41−54.
Craik, D. J., & Higgins, K. (1989) *Annu. Rep. NMR Spectrosc. 22*, 61.
Foote, J., & Milstein, C. (1994) *Proc. Natl. Acad. Sci. U.S.A. 91*, 10370−10374.
Gearhart, P. J., Sigal, N. H., & Klinman, N. R. (1975) *J. Exp. Med. 141*, 56−71.
Gerig, J. T. (1989) *Methods Enzymol. 177*, 3−23.
Glaudemans, C. P., Lerner, L., Daves, G. D., Jr., Kov'ac, P., Venable, R., & Bax, A. (1990) *Biochemistry 29*, 10906−10911.
Harris, R. K. (1986) *Nuclear magnetic resonance spectroscopy. A physicochemical view*, Longman Scientific & Technical, Essex, England.
Innis, M. A., & Gelfand, D. H. (1990) *PCR Protocols: A guide to methods and applications*, pp 1−20, Academic Press, Inc., San Diego, CA.
Johnson, S., & Bird, R. E. (1991) *Methods Enzymol, 203*, 88−98.
Kabat, E. A., Wu, T. T., Reid-Miller, M., Perry, H. M., & Gottesman, K. S. (1987) *Sequences of Proteins of Biological Interests*, NIH, Bethesda, MD.
Kooistra, D. A., & Richards, J. H. (1978) *Biochemistry 17*, 345−351.
Kumar, A., Ernst, R. R., & Wüthrich, K. (1980) *Biochem. Biophys. Res. Commun.*, 1−6.
Lanzavecchia, A. (1990) *Annu. Rev. Immunol. 8*, 773−793.
Marion, D., & Wüthrich, K. (1983) *Biochem. Biophys. Res. Commun. 113*, 967−974.
Odaka, A., Kim, J. I., Takahashi, H., Shimada, I., & Arata, Y. (1992) *Biochemistry 31*, 10686−10691.
Rance, M., Sørensen, O. W., Bodenhausen, G., Wagner, G., Ernst, R. R., & Wüthrich, K. (1983) *Biochem. Biophys. Res. Commun. 117*, 479−485.
Rodwell, J. D., Gearhart, P. J., & Karush, F. (1983) *J. Immunol. 130*, 313−316.
Sandström, J. (1982) *Dynamic NMR spectroscopy*, Academic Press, New York.
Stenzel-Poore, M. P., & Rittenberg, M. B. (1991) *Somatic Hypermutation*, pp 95−104, CRC Press, Boca Raton, FL.
Takahashi, H., Suzuki, E., Shimada, I., & Arata, Y. (1992) *Biochemistry 31*, 2464−2468.
Theriault, T. P., Leahy, D. J., Levitt, M., McConnell, H. M., & Rule, G. S. (1991) *J. Mol. Biol. 221*, 257−270.
Turner, A. F., & Khorana, H. G. (1959) *J. Am. Chem. Soc. 81*, 4651−4656.

BI950823E